Symmetry-protected TM modes in rib-like, plus-shaped optical waveguides with shallow etching

Necati Üstün, Henna Farheen, Manfred Hammer, Jens Förstner*

Theoretical Electrical Engineering, Paderborn University, Paderborn, Germany

Abstract: Lateral leakage of TM modes in dielectric optical waveguides of rib/ridge or strip-loaded types can be fully suppressed, if the waveguide core is formed not through a strip that protrudes at one side (up) from the remaining lateral guiding slab, but through parallel strips on both sides (up and down), such that the resulting cross section becomes vertically symmetric. The fairly general arguments underlying the leakage suppression apply to TM modes of all orders simultaneously, and are independent of wavelength. These plus-shaped waveguides support strictly guided, non-leaky TM modes for, in principle, arbitrarily shallow etching.

Keywords: photonics, integrated optics, rib waveguides, strip-loaded waveguides, shallow etching, guided modes, magical widths, leakage losses.

1 Introduction

Integrated photonic circuits often rely on dielectric waveguides of rib or ridge type, for establishing connections between components and as basic elements for the construction of functional components. In many cases these channels are dimensioned in regimes of shallow etching, with low rib height and a lateral layer stack with a central high-index core layer. The shape is illustrated in Fig. 1(a). The channels then typically support strictly guided, lossless TE modes, while the TM modes exhibit more or less pronounced lateral leakage. The leakage effect has been observed and explained in several instances [1–9]. The respective waveguides can still be highly useful, mainly due to their low loss properties [10, 11], but are mostly restricted to the propagation of TE modes only. These notions apply also to strip-loaded waveguides, where the strip consists of another material, mostly with lower refractive index than that of the core layer.

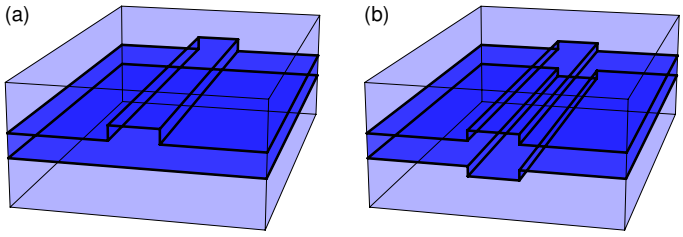

Figure 1: Standard dielectric rib waveguide (a), and the "plus" configuration (b), schematically. A structured central core layer is sandwiched between identical (here) substrate and cover media.

With this paper, we highlight a straightforward way to prevent the lateral leakage in rib like waveguides with shallow etching, by changing the cross section towards the shape of Fig. 1(b). As we shall see, the vertical symmetry effectively suppresses the TM-to-TE coupling at the rib sidewalls, and thus the leakage of the TM modes. For lack of a better term we choose the name *plus waveguides* for channels with this cross section shape, with co-aligned ribs of the same size protruding both upward and downward from the central core layer.

Assuming that a major part of propagation losses originates from rough sidewalls [12, 13], low attenuation can be expected for the modes of shallow plus waveguides with their small sidewall area, just as for standard rib configurations. Certain applications, however, e.g. the manipulation of photon pairs in quantum optics [14, 15], require modes of both fundamental polarizations to be guided. Low losses, and the adequate management of leakage, are of importance also in the area of thin-film lithium niobate (TFLN) or lithium-niobate on insulator (LNOI) photonic circuits [16, 17], although there might be scenarios where guidance of only one polarization is advantageous [18]. Further, rib waveguides with shallow etching, and thus our plus structures, can play a role

*Paderborn University, FG Theoretical Electrical Engineering Warburger Straße 100, 33098 Paderborn, Germany
Phone: ++49(0)5251/60-3560 Fax: ++49(0)5251/60-3524 E-mail: manfred.hammer@uni-paderborn.de

in the field of integrated photonic circuits based on semi-guided waves [19–21], for the excitation and detection of on-chip semi-guided optical beams [22, 23].

In Section 2 we review briefly the mechanisms that lead to lateral leakage in traditional rib structures, and then argue how the symmetry property protects the TM modes in the plus configuration. The statements are illustrated with a series of numerical examples in Section 3. These include standard ribs with their "magical" widths [7], comparable plus waveguides that support strictly guided, lossless TM modes for *any* width, and a brief assessment of tolerances for the potential fabrication of plus waveguides.

2 Channels with guiding lateral layers

We consider waveguides with the cross sections of Fig. 2. For easier comparison, the parameters w for rib width, h for the total etching depth, and t for the total thickness of the non-etched film in the core region are used for both types. Identical values describe waveguides with the same core area. While the plus configuration is fully symmetric with respect to the plane $x = 0$ ("vertically symmetric"), the rib waveguide is not.

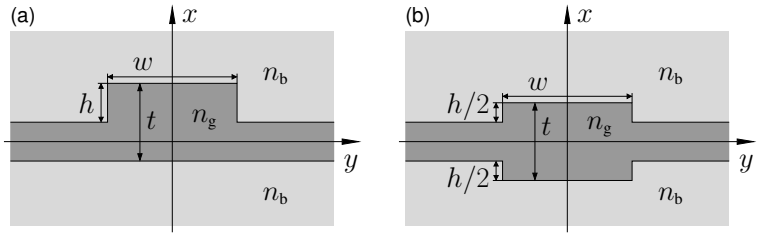

Figure 2: Waveguide configurations with rib- (a) and plus geometries (b). A guiding film of total thickness t with refractive index n_g is embedded in a background medium with refractive index n_b. Upper and lower ribs of width w and etching heights h, or $h/2$, respectively, provide lateral confinement. Cartesian coordinates x and y are oriented as shown in the figures, with the origin in the middle of the laterally remaining film. Waves propagate in the z direction (not shown).

For the following arguments we adopt a frequency domain description. The optical electromagnetic fields $\boldsymbol{E}$ and $\boldsymbol{H}$ depend on time as $\sim\exp(\mathrm{i}\omega t)$, with angular frequency $\omega = k\mathrm{c} = 2\pi\mathrm{c}/\lambda$, vacuum speed of light c, wavenumber k, and wavelength λ. While we use material parameters for lossless media, due to lateral leakage the modes of interest are potentially lossy. This is expressed through complex propagation constants, with real phase constants $\beta = kN_{\mathrm{eff}}$, effective index N_{eff}, and real attenuation constants α. For propagation in positive z-direction, the electromagnetic fields depend on z as $\sim\exp(-\mathrm{i}(\beta - \mathrm{i}\alpha)z)$. The optical power associated with the propagation of a single mode then decays as $\sim\exp(-2\alpha z)$, such that the power loss LO in decibel units per distance is $\mathrm{LO}/z = 20\,\alpha/\ln(10)$.

The concepts require vertically symmetric layer stacks, with a guiding film of refractive index n_g between half-infinite substrate and cladding regions of refractive index n_b. We adopt typical parameters from silicon photonics [24]. Values $n_g = 3.45$, $n_b = 1.45$ relate to a silicon film in a silica background at a typical telecom wavelength of $\lambda = 1.55\,\mu$m. Further, we shall restrict the discussion to vertically single mode channels with a total film thickness $t = 220\,$nm. While all waveguides support also non-leaky fundamental and, depending on the rib width, higher order TE modes, for this paper we focus on the TM polarized modes only.

2.1 Slab modes, dispersion properties

The modes of the rib and plus channels can be viewed as local superpositions of the slab modes of the central and lateral layer stacks. This is a rigorous approach: Normal mode expansions [25], including guided modes as well as a discrete set of radiation modes on a computational x-interval of suitable size (convergence), form a basis for respective eigenproblem solvers (film mode matching, [7, 8, 26–28]), or solvers for the related scattering problems [29].

Hence, as a starting point for the following reasoning, Fig. 3 shows the results of a slab mode analysis [30] of the present symmetric three-layer stack, for varying thickness d of the core layer. At the level $d = t$ of the thickness of the non-etched film in the later channel waveguides, only the fundamental TE and TM slab modes are supported, with effective indices $n(\mathrm{TE0}, t)$ and $n(\mathrm{TM0}, t)$. These levels, relative to effective indices of modes of both polarizations at the lower thickness $d = t - h$ of the etched regions, will become relevant in the next section.

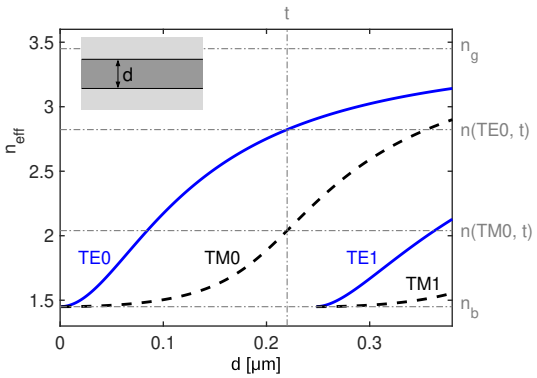

Figure 3: Symmetric three layer slab waveguides with refractive index profile $n_\mathrm{b} : n_\mathrm{g} : n_\mathrm{b}$, with $n_\mathrm{b} = 1.45$, $n_\mathrm{g} = 3.45$ at wavelength $\lambda = 1.55\,\mu\mathrm{m}$, effective indices n_eff versus the core layer thickness d, curves relate to TE and TM modes of 0th and 1st order. At the thickness $d = t = 220\,\mathrm{nm}$, the slab supports fundamental TE and TM modes with effective indices $n(\mathit{TE0}, t) = 2.823$ and $n(\mathit{TM0}, t) = 2.040$.

Further, the effective indices of TM slab modes limit the range of effective indices N_eff, where TM modes are supported by the rib and plus channels. The former value $n(\mathrm{TM0}, t)$ forms an upper limit. The lower limit is given by the effective index $n(\mathrm{TM0}, t-h)$ of the fundamental TM mode of the thinner external region of the channel. Respective levels $n(\mathrm{TM0}, 220\,\mathrm{nm}) = 2.040$, $n(\mathrm{TM0}, 195\,\mathrm{nm}) = 1.851$, $n(\mathrm{TM0}, 170\,\mathrm{nm}) = 1.702$, $n(\mathrm{TM0}, 120\,\mathrm{nm}) = 1.537$ for the examples of Sections 3.1 and 3.2 are indicated in Figs. 4 and 7.

2.2 Lateral leakage

The leakage of our rib waveguides can be understood as a partly laterally outwards directed transport of power through slab eigenmodes of the thinner, etched regions outside the core. Assume that the channel supports a mode with propagation constant $\beta = kN_\mathrm{eff}$. Its electromagnetic mode profile can be expanded into complete sets of normal slab modes [25, 29], separately for the regions $y < -w/2$, $-w/2 < y < w/2$, and $y > w/2$ of constant core layer thickness. In the external regions these need to be unidirectional expansions, where only slab modes contribute, that either propagate or decay outwards (corresponding to transparent boundary conditions at a distance left and right of the rib). By construction, all terms in the expansions (vectorial "oblique modes" [29]) share the exponential dependence $\sim\exp(-\mathrm{i}\beta z)$ of the channel mode. While these modes satisfy orthogonality relations with respect to suitable mode products [25, 31, 32] if they are supported by the same layer stack, TE and TM modes of slabs of different thickness are *not* orthogonal (i.e. the modes "couple") in that sense.

To determine whether the channel mode is potentially leaky, we look at the slab mode expansions in one of the external regions, say for $y > w/2$. Here it needs to be decided, whether the sum field includes terms that could potentially transport power in $+y$-direction. Hence we examine each of the slab modes in turn.

In case of an evanescent mode, power transport is not possible in this context of unidirectional expansions. We can thus restrict to propagating slab modes, with real effective indices n_eff, in the region $y > w/2$. As part of the overall field of the channel mode, each such mode travels in the y-z-plane with wavenumber kn_eff and wavevector (k_y, β), where its propagation in y-direction is governed by the wavenumber $k_y = \sqrt{k^2 n_\mathrm{eff}^2 - \beta^2}$.

For a slab mode with effective index $n_\mathrm{eff} < \beta/k = N_\mathrm{eff}$ below the level of the channel mode, k_y is imaginary. The slab mode exhibits evanescent field behavior along the lateral y-axis. There is no power transport, and hence no lateral leakage, associated with that wave.

If, on the other hand, k_y turns out to be real for the slab mode under scrutiny, that mode can transport optical power along the y-direction, and, consequently, can potentially contribute to the leakage of the channel mode. This applies to all slab modes with effective indices $n_\mathrm{eff} > N_\mathrm{eff}$ higher than the effective index assumed for the channel mode. In case the net contribution of these slab modes (both polarizations, $+y$ and $-y$ directions) to the leakage comes out as nonzero, our initial assumption of a real propagation constant is violated; the channel does not support a guided mode at this level of N_eff.

In the present isotropic symmetric three-layer slabs, the highest effective index of all modal solutions is always found for the guided TE mode. Consulting Fig. 3, an interval $[n(\mathrm{TE0}, t-h), n(\mathrm{TE0}, t)]$ for effective indices of potential guided channel modes opens up for all etching depths h. Consequently, the rib waveguides always support a guided TE mode, irrespectively of their width and etching depth.

For TM modes, the former reasoning suggests several approaches that could lead to a suppression of leakage. In the first place, the effective index maximum of the slab modes in the external regions could be lowered,

by increasing the etching depth. According to Fig. 3, this requires an etching depth with $n(\mathrm{TE0}, t-h) < n(\mathrm{TM0}, t)$, or $h > 136\,\mathrm{nm}$, for the present parameters, such that one leaves the regime of shallow etching. For rib waveguides in that regime, the leakage of TM modes with $n(\mathrm{TM0}, t-h) < N_{\mathrm{eff}} < n(\mathrm{TM0}, t) < n(\mathrm{TE0}, t-h)$ can be attributed exclusively to the fundamental TE modes in the thinner outer regions. As an alternative to deep etching, the contributions of these waves to the leakage can be made to cancel out. One is thus led to the "magical widths" [1,5,7,9], where guided TM modes are supported for specific rib widths only. Respective configurations are also discussed with a view to "bound states in the continuum" (BIC, [33–35]).

As a third alternative, the excitation of these lateral TE slab modes can be prevented by force of symmetry, i.e. by stepping from the rib to a plus configuration. This can be realized as follows. All slab modes supported by the present symmetric layer stacks are symmetric in a specific sense. Depending on polarization and order, the electric and magnetic components of the mode profiles are either of even or odd parity with respect to the central horizontal mirror plane at $x = 0$. Vanishing components can be counted as either even or odd. Table 1 summarizes these properties. The same signs in the columns of y- and z-components for electric and magnetic fields indicate that these symmetry conditions hold as well, if, in the assembly of the channel modes, the slab modes are superimposed for in-plane oblique angles of propagation.

	E_x	E_y	E_z	H_x	H_y	H_z	
$\mathrm{PMC}_{x=0}$	$-$	$+$	$+$	$+$	$-$	$-$	TE0, TM1, ...
$\mathrm{PEC}_{x=0}$	$+$	$-$	$-$	$-$	$+$	$+$	TM0, TE1, ...

Table 1: Boundary condition in the plane $x = 0$, parity of field profile components (even: $+$, odd: $-$), and associated identifiers of slab modes.

The symmetry of the fields in the plane $x = 0$ corresponds to boundary conditions of either PMC or PEC type ("perfect magnetic / electric conductor"), as indicated in the table. Due to the symmetry of the full plus waveguide structure, also the modal solution for the channel waveguide satisfies either PMC or PEC conditions on the plane $x = 0$. Slab modes with differing parity cannot contribute to that solution. Specifically, the profiles of all TM polarized channel modes satisfy PEC conditions in the plane $x = 0$ (Note that we consider vertically single mode waveguides only). According to Table 1, the TE0 modes in the lateral slabs are of opposite parity (PMC conditions). As such, these cannot contribute to the TM channel modes, which become strictly guided. Accepting standard idealizations, the modes are lossless.

Alternatively, this can also be seen in the coupling between slab modes associated with the interior and exterior regions. That interaction can be quantified through the overlaps of mode profiles, in terms of the following product [31, 32] of slab modes with electromagnetic profiles $(\boldsymbol{E}_1, \boldsymbol{H}_1)$ and $(\boldsymbol{E}_2, \boldsymbol{H}_2)$:

$$\langle \boldsymbol{E}_1, \boldsymbol{H}_1; \boldsymbol{E}_2, \boldsymbol{H}_2 \rangle = \frac{1}{4} \int (E_{1z}^* H_{2x} - E_{1x}^* H_{2z} + E_{2z} H_{1x}^* - E_{2x} H_{1z}^*)\, \mathrm{d}x\,. \tag{1}$$

Here the asterisk denotes complex conjugation. Note that we need to consider interaction across interfaces in the x-z-plane, i.e. propagation of slab modes in $\pm y$-direction. According to Table 1, all terms in the overlaps (1) of TE0 and TM0 modes combine components with opposite parity, such that the integrals vanish.

A hint to this mechanism of suppressing TE/TM interaction, but no continuing exploration, can be found in Ref. [9]. Respective symmetry arguments play a role in the discussion of leaky slot waveguides in Ref. [36], and have been applied to related scattering problems for semi-guided waves in Refs. [37–39], also concerning the existence of BIC states [34]. Earlier, a symmetric, weakly guiding waveguide structure similar to the present plus configuration has been considered on the basis of a scalar Helmholtz equation [40], as a means to realize BIC states. Symmetry protected BIC states could be observed in a plus-shaped array of waveguide channels [41].

3 Modal properties of channels with shallow etching

The numerical results in this section rely on the fully vectorial finite-element based eigensolvers of the COMSOL [42] and JCMwave [43] software suites. The tools are applied with converged mesh settings (COMSOL), or with adaptive mesh refinement enabled (JCMwave). Their outcome coincides, on the scale of the figures and as far as observed. The modal fields of Figs. 5 and 6 are computed on a 2-D computational window $(x, y) \in [-1.4, 1.4] \times [0, 3]\ \mu\mathrm{m}^2$, where left-right modal symmetry has been exploited by PMC or PEC conditions at the western boundary at $y = 0$. Further PEC conditions enclose the computational domain at its south-

ern and northern boundaries, while perfectly matched layers (COMSOL) or transparent conditions (JCMwave) are applied on the remaining eastern boundary. The computational settings required for converged results differ for the parameter scans elsewhere in the paper.

3.1 Conventional rib waveguides

Fig. 4 summarizes results for a series of rib waveguides as in Fig. 2(a), with varying rib width and etching depth. One observes a fairly standard dependence of effective indices on w and h, with modes of higher orders appearing with growing core area. With singular exceptions, the TM modes are leaky for all shown configurations.

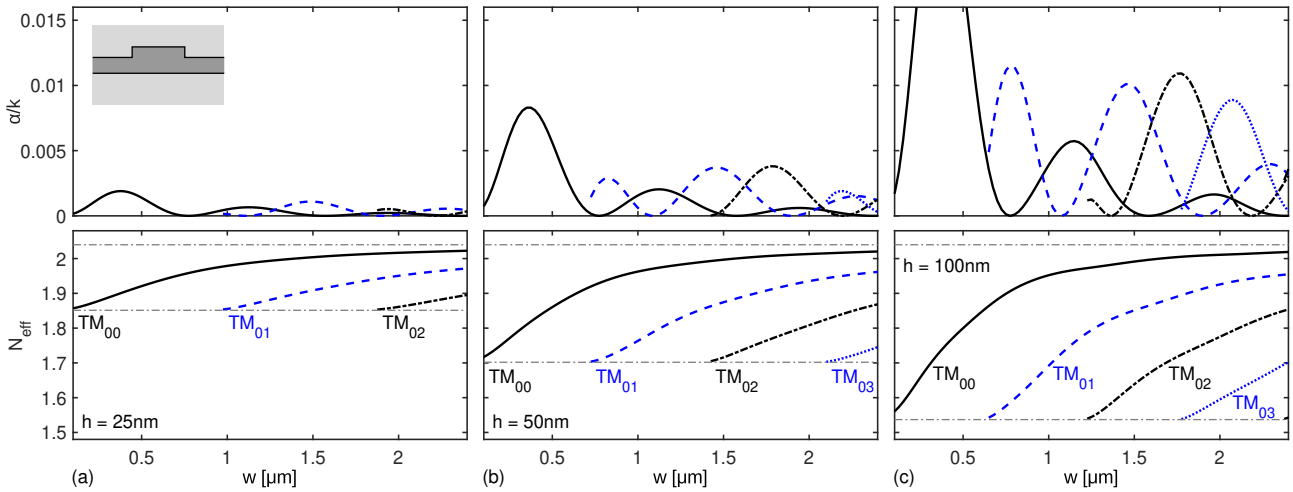

Figure 4: Effective indices N_{eff} (bottom) and attenuation constants α (top) of TM modes versus the rib width w, for rib waveguides with the parameters of Fig. 2(a), for etching depths $h = 25\,\text{nm}$ (a), $h = 50\,\text{nm}$ (b), and $h = 100\,\text{nm}$ (c).

The oscillatory behavior of the attenuation on rib width, and the occurrence of "magical widths" with zero leakage, can be explained along a line of arguments (see e.g. Ref. [9] for details) on the interference of TE-polarized slab modes, propagating at oblique angles inside and outside the core region of the rib waveguide. These waves are excited at both sidewalls of the rib, traveling at angles, in the x-z-plane, in both the positive and negative y-direction. Depending on the distance of the excitation points, i.e. on the rib width, the waves interfere in the regions outside the rib with varying phase. Due to the left-right symmetry of the configuration, full destructive interference is possible at certain rib widths, leading to a cancellation of the leakage.

In line with that reasoning, in Fig. 4 one observes different magical widths for the TM modes of different orders. For our parameters, the lowest instance for the TM_{00}-mode appears at roughly $w = 0.77\,\mu\text{m}$, where the channels for $h = 50\,\text{nm}$ and $h = 100\,\text{nm}$ support TM_{01}-modes already, with their leakage roughly at a maximum at this width.

Leakage losses associated with ribs of larger etching depth h are found to be, in general, higher than those of ribs with more shallow etching. To a degree this can be understood by accepting that the leakage process is driven by the relative electric field strength, at the positions of the sidewalls, of the TM mode profile in question. For shallow etching, the then wide field is low at the sidewalls. With growing etching depths and growing lateral mode confinement, the local field at these interfaces increases. Once this comes close to causing true guiding, the profiles become more limited to the range of the rib, and the relative field at the sidewalls decreases again, leading to a rapid drop in leakage down to zero (graphs not shown here).

Next, with Fig. 5(a–c) we take a look at the field profiles associated with the leaky TM_{00} mode in a rather arbitrarily chosen intermediate single mode (non-magic) rib configuration for $w = 0.5\,\mu\text{m}$ and $h = 50\,\text{nm}$. For these plots, the overall phase of each mode profile has been adjusted such that the electric component E_x becomes real at the position of its largest field strength. Besides that major E_x component, one observes the smaller components E_z and E_y of the vectorial, hybrid mode field. Both components can be associated with outwards traveling TE slab modes, propagating at oblique angles. The leakage shows up as the oscillatory waves in the slab regions left and right of the rib.

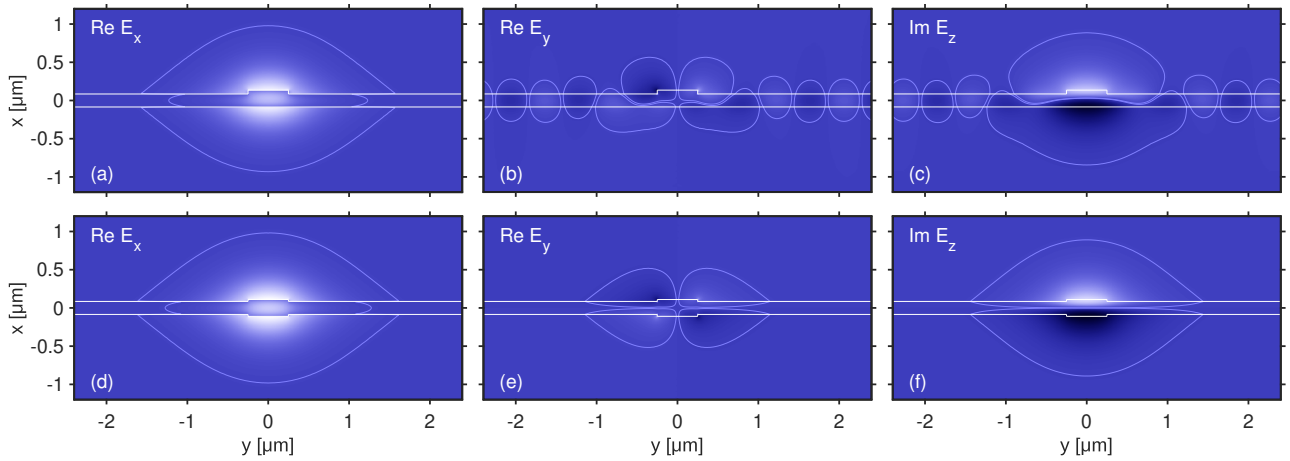

Figure 5: Fundamental TM mode of a rib (a–c) and plus waveguide (d–f) according to Fig. 2, with $h = 50\,\mathrm{nm}$ and $w = 0.5\,\mu\mathrm{m}$; effective indices and attenuation constants are $N_{\mathrm{eff}} = 1.8604$, $\alpha/k = 0.0056$ (rib) and $N_{\mathrm{eff}} = 1.8616$, $\alpha = 0$ (plus). Real parts $\mathrm{Re}\,E_x$ (a, d), $\mathrm{Re}\,E_y$ (b, e) of the transverse and imaginary parts $\mathrm{Im}\,E_z$ (c, f) of the longitudinal electric profile components are shown. Color scales are comparable within each row; single contours indicate levels of $\pm 1\%$ of the overall field maximum.

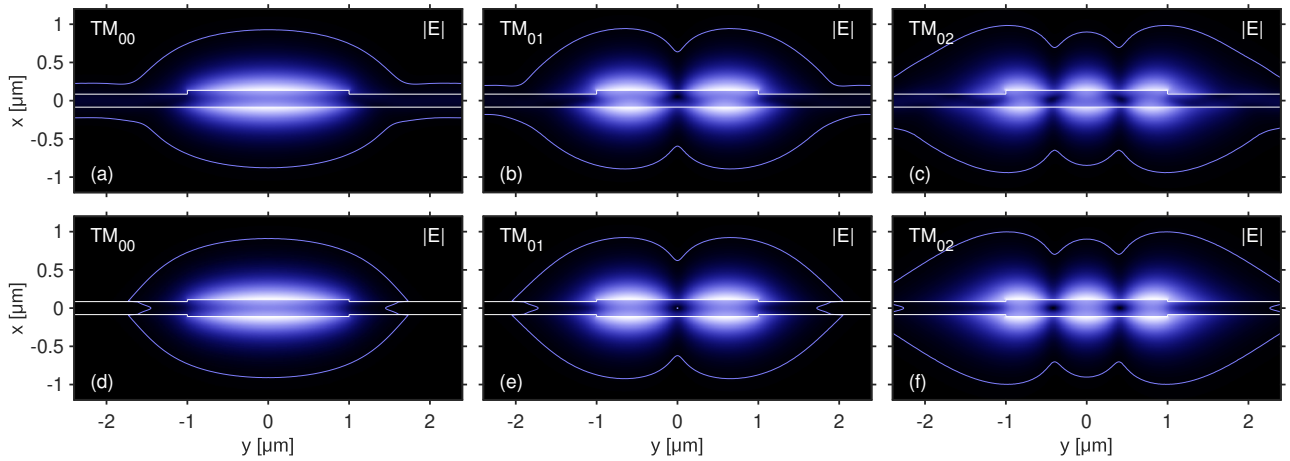

Figure 6: TM modes supported by a rib waveguide (a–c) and plus waveguide (d–f) according to Fig. 2, with $h = 50\,\mathrm{nm}$ and $w = 2.0\,\mu\mathrm{m}$. The panels show the absolute value $|\boldsymbol{E}|$ of the electric profile for the modes of fundamental (a, d), first (b, e), and second order (c, f). Pairs of effective indices and attenuation constants $[N_{\mathrm{eff}}, \alpha/k]$: $[2.0131, 0.0006]$ (rib, TM_{00}), $[1.9351, 0.0003]$ (rib, TM_{01}), $[1.8083, 0.0016]$ (rib, TM_{02}), and $[2.0130, 0]$ (plus, TM_{00}), $[1.9339, 0]$ (plus, TM_{01}), $[1.8092, 0]$ (plus, TM_{02}). Modes are power normalized; single contours indicate levels of 1% of the overall field maximum, with color scales adjusted separately for each plot.

Fig. 6(a–c) illustrates TM modes of higher orders, supported by a wider multimode rib of width $w = 2\,\mu\mathrm{m}$, again for $h = 50\,\mathrm{nm}$. In the absolute electric field profiles, the leakage becomes apparent merely in the left- and right-extending low level contours.

3.2 Plus waveguides

Eigenmode calculations for comparable plus waveguides lead to the results shown in Fig. 7. The channels support TM modes with effective indices that are very close, but not identical, to the values for rib waveguides in Fig. 4. In accordance with Section 2, the numerical simulations predict vanishing attenuation constants for all plus configurations (within the accuracy margins, not visible on the scale of Fig. 4).

The comparison of field shapes between rib- and plus channels in Figs. 5 and 6 shows similar mode profiles, with, apart from the vertical shift, matching dominant electric field profiles E_x. Differences appear in the minor profile components E_y and E_z, where the leakage-related lateral oscillations are absent for the strictly guided TM modes of the plus waveguides.

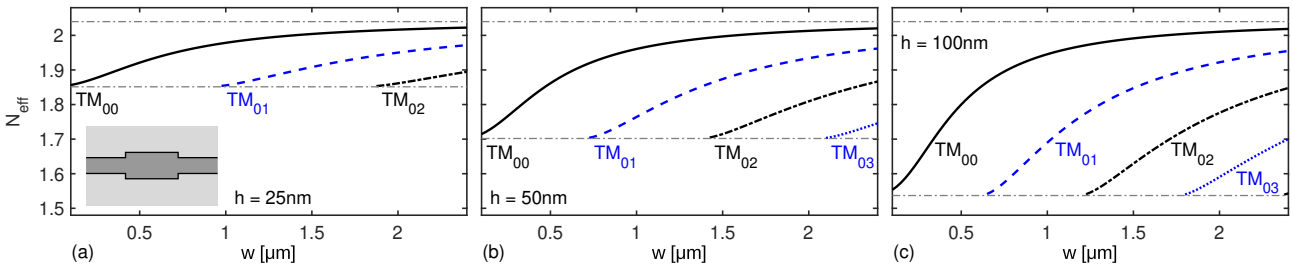

Figure 7: Effective indices N_{eff} of guided TM modes as a function of width w, for plus waveguides with the parameters of Fig. 2(b), for etching depths $h = 25\,\text{nm}$ (a), $h = 50\,\text{nm}$ (b), and $h = 100\,\text{nm}$ (c).

3.3 Channels with partly vertical symmetry

Leakage suppression in the former plus waveguide relies on the strict symmetry of the waveguides. Necessarily, actual fabricated devices will realize that property only with a certain accuracy. Imagining a fabrication procedure based on repeated steps of layer deposition, mask application, and etching processes, among the many things that can potentially go wrong are errors in etching depth, errors in feature width, and errors in mask alignment. To assess these effects, three deviation parameters Δh, Δw, and Δp are introduced in Fig. 8, in such a way to keep the overall "core area" roughly constant.

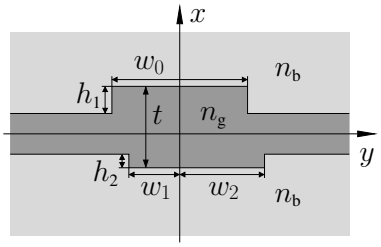

Figure 8: In general not symmetric waveguide close to the plus geometry. Parameters are as given in Fig. 2, with constrained additional lengths $h_1 = h/2 + \Delta h$, $h_2 = h/2 - \Delta h$, $w_0 = w + \Delta w$, $w_1 = w/2 - \Delta w/2 - \Delta p$, $w_2 = w/2 - \Delta w/2 + \Delta p$.

Δh then measures the deviation in rib heights, with extremal values $\Delta h = \pm h/2$ (rib waveguides). Δw introduces an asymmetry in the widths of the upper and lower ribs, and Δp covers a relative lateral shift of these ribs. In all cases, zero deviations indicate the strictly symmetric plus waveguide. We focus on single mode configurations with a rib width $w = 0.5\,\mu\text{m}$, with the different etching depths $h \in \{25, 50, 100\}\,\text{nm}$ as considered for Fig. 7. Fig. 9 shows the properties of the fundamental TM mode as functions of the three deviation parameters (only one of these is nonzero at a time).

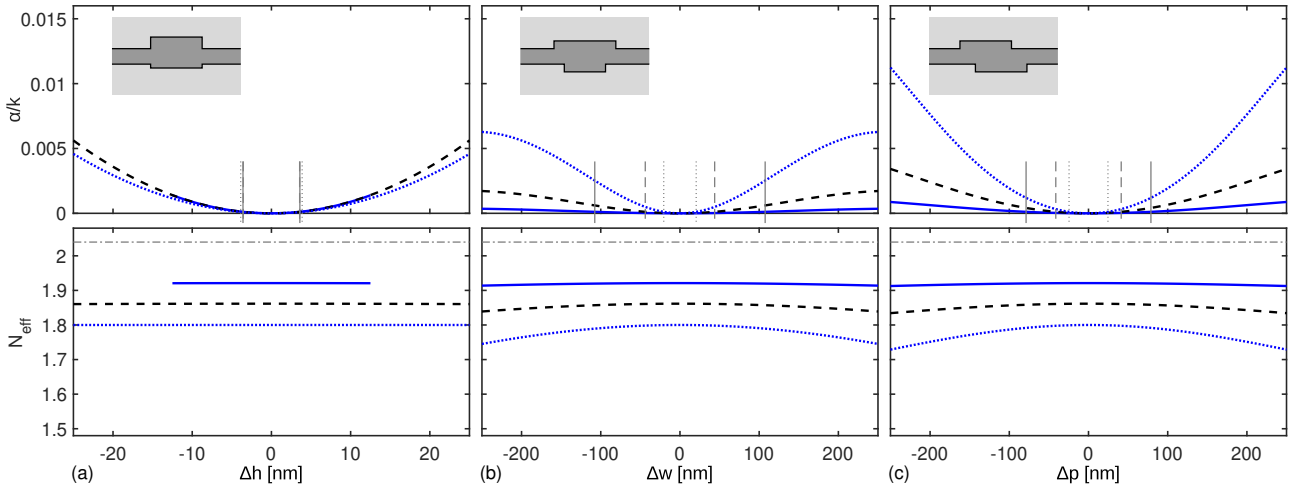

Figure 9: Plus waveguides with deformations according to Fig. 8; effective indices N_{eff} (bottom) and attenuation constants α (top) of fundamental TM modes as function of the perturbation strength. Differences Δh in etching depths (a), differences Δw in rib widths (b), and lateral shifts Δp of the rib positions have been considered, for original channels according to Fig. 2(b), with $w = 0.5\,\mu\text{m}$ and $h = 25\,\text{nm}$ (solid), $h = 50\,\text{nm}$ (dashed), and $h = 100\,\text{nm}$ (dotted lines). The short vertical lines (styles correspond to etching depths) mark tolerance intervals: For deformation parameters within these limits, the attenuation and loss of the TM$_{00}$ mode are lower than $1.15 \cdot 10^{-4}\,\mu\text{m}^{-1}$ or $1\,\text{dB}/\,\text{mm}$, respectively.

While, on the scale of the figures, the deformations hardly affect the effective indices of the modes, all types of perturbation introduce attenuation that is noticeable on the scale of Fig. 4. Note, however, that we here consider rather large "errors": The maximum values Δh (not shown for $h = 100\,\text{nm}$) correspond to the traditional rib configuration with absent lower or upper rib; $\Delta w = \pm 250\,\text{nm}$ indicates a structure where the upper rib is three times as wide as the lower one, and for $\Delta p = \pm 250\,\text{nm}$, the ribs overlap with half their width only.

For a somewhat more quantitative assessment, we have evaluated tolerance intervals such that the loss associated with the fundamental TM modes remains below a level of $1\,\text{dB}/\,\text{mm}$, or the attenuation constants below $1.15 \cdot 10^{-4}\,\mu\text{m}^{-1}$. Respective intervals are indicated in Fig. 9. These can be compared with the attenuation curves of Fig. 4 for standard rib channels: For the loss of the TM_{00} modes to be below $1/\,\text{dB}/\,\text{mm}$, the rib width w must be kept within intervals (full widths) of roughly $161\,\text{nm}$ ($h = 25\,\text{nm}$), $83\,\text{nm}$ ($h = 50\,\text{nm}$), and $52\,\text{nm}$ ($h = 100\,\text{nm}$), around the narrowest "magical widths". The width-related parameters Δw and Δp for the generalized plus configurations are thus observed to be of a sensitivity similar to the width parameter in case of the "magical" rib waveguides.

Other types of deviations from the ideal rectangular plus configuration can be considered. Among these are e.g. differences in thickness of the left and right exterior slab regions [34], or non-vertical, slanted sidewalls [44]. The arguments leading to the suppression of lateral leakage remain valid, as long as the overall channel is mirror symmetric with respect to the central horizontal plane at $x = 0$. Left-right mirror symmetry with respect to $y = 0$ is not required. Leakage must be anticipated, if the fabrication steps for the lower and upper ribs lead to pronouncedly different sidewall tilt angles. Our emphasis, however, is on structures with *shallow etching*, where the influence of the precise sidewall shapes can be expected to be small, when compared to the x-positioning of the wide central and outer horizontal core interfaces.

4 Concluding remarks

The leakage of TM modes in shallow rib or ridge waveguides can be suppressed, if the channels are formed with two identical, co-aligned ribs on both sides of the core layer. Strictly guided TM modes are supported, for in principle arbitrarily narrow channels, and arbitrarily shallow etching. The mechanism relies only on the properties of the slab modes in the central and lateral regions of the rib, and on their symmetry. Hence, strict suppression of leakage should also be possible e.g. for waveguides with slanted sidewalls, or for waveguides of graded-index types, as long as the full structure remains vertically symmetric. While our present examples concern high-contrast Si/SiO_2-waveguides, all arguments should apply just as well for photonic platforms with lower refractive index contrast.

In case the symmetry is violated, the leakage protection mechanism breaks down manageably. We have quantified the effects of different types of non-symmetry for a few single mode channels. Tolerances comparable to rib waveguides, operated at magic widths, have been observed. If acceptable for the application at hand, a plus waveguide at magic width could probably show even less critical tolerances (not evaluated in this paper).

Obviously, when compared to standard rib waveguides, the plus configuration requires a more complex fabrication procedure for the guiding layer, and also a cover layer to realize the vertical symmetry. The magical widths, however, depend on modal effective indices of the slab modes involved, and are consequently wavelength dependent. In contrast, for the plus waveguides, the symmetry arguments remain valid at arbitrary wavelengths, as long as the modes in question are supported. Such a broadband mechanism might be of particular relevance for applications that include nonlinear processes, where the channels need to support guided modes at grossly unequal (pump, signal) wavelengths.

Further, in a rib waveguide at a specific magical width, in general leakage is suppressed for one particular TM mode only. Contrarily, the symmetry protection of plus waveguides works simultaneously for TM modes of all orders. Depending on whether the application in question requires the presence of higher order modes, this can be a strong advantage, such as for an interferometer relying on multimode interference (MMI). Nevertheless it is always possible to restrict the number of guided TM modes by choosing an appropriate maximum width of the plus waveguide.

Funding

Financial support from the German Research Foundation (Deutsche Forschungsgemeinschaft DFG, project 231447078–TRR 142, subproject B06) and from the Ministry of Culture and Science of the state of North Rhine-Westphalia (project PhoQC) is gratefully acknowledged.

Disclosures

The authors declare no conflicts of interest.

Data availability

Data underlying the results presented in this paper are not publicly available at this time but may be obtained from the authors upon reasonable request.

References

[1] K. Ogusu, S. Kawakami, and S. Nishida. Optical strip waveguide: an analysis. *Applied Optics*, 18(6):908–914, 1979.

[2] K. Ogusu and I. Tanaka. Optical strip waveguide: an experiment. *Applied Optics*, 19(19):3322–3325, 1980.

[3] S.-T. Peng and A. Oliner. Guidance and leakage properties of a class of open dielectric waveguides: Part I — mathematical formulations. *IEEE Transactions on Microwave Theory and Techniques*, MTT-29(9):843–854, 1981.

[4] A. Oliner, S.-T. Peng, T.-I. Hsu, and A. Sanchez. Guidance and leakage properties of a class of open dielectric waveguides: Part II — new physical effects. *IEEE Transactions on Microwave Theory and Techniques*, MTT-29(9):855–869, 1981.

[5] K. Ogusu. Optical strip waveguide: a detailed analysis including leaky modes. *Journal of the Optical Society of America*, 73(3):353–357, Mar 1983.

[6] M. A. Webster, R. M. Pafchek, A. Mitchell, and T. L. Koch. Width dependence of inherent TM-mode lateral leakage loss in silicon-on-insulator ridge waveguides. *IEEE Photonics Technology Letters*, 19(6):429–431, 2007.

[7] T. G. Nguyen, R. S. Tummidi, T. L. Koch, and A. Mitchell. Rigorous modeling of lateral leakage loss in SOI thin-ridge waveguides and couplers. *IEEE Photonics Technology Letters*, 21(7):486–488, 2009.

[8] X. Xu, S. Chen, J. Yu, and X. Tu. An investigation of the mode characteristics of SOI submicron rib waveguides using the film mode matching method. *Journal of Optics A: Pure and Applied Optics*, 11(1):015508, 2008.

[9] T. G. Nguyen, A. Boes, and A. Mitchell. Lateral leakage in silicon photonics: Theory, applications, and future directions. *IEEE Journal of Selected Topics in Quantum Electronics*, 26(2):1–13, 2020.

[10] M. A. Webster, R. M. Pafchek, G. Sukumaran, and T. L. Koch. Low-loss quasi-planar ridge waveguides formed on thin silicon-on-insulator. *Applied Physics Letters*, 87(23):231108, 2005.

[11] P. Dong, W. Qian, S. Liao, H. Liang, C.-C. Kung, N.-N. Feng, R. Shafiiha, J. Fong, D. Feng, A. V. Krishnamoorthy, and M. Asghari. Low loss shallow-ridge silicon waveguides. *Optics Express*, 18(14):14474–14479, 2010.

[12] D. Melati, A. Melloni, and F. Morichetti. Real photonic waveguides: guiding light through imperfections. *Advances in Optics and Photonics*, 6(2):156–224, 2014.

[13] S. M. Lindecrantz and O. G. Hellesø. Estimation of propagation losses for narrow strip and rib waveguides. *IEEE Photonics Technology Letters*, 26(18):1836–1839, 2014.

[14] H. Herrmann, X. Yang, A. Thomas, A. Poppe, W. Sohler, and C. Silberhorn. Post-selection free, integrated optical source of non-degenerate, polarization entangled photon pairs. *Optics Express*, 21(23):27981–27991, 2013.

[15] P. R. Sharapova, K. H. Luo, H. Herrmann, M. Reichelt, T. Meier, and C. Silberhorn. Toolbox for the design of $LiNbO_3$-based passive and active integrated quantum circuits. *New Journal of Physics*, 19(12):123009, 2017.

[16] E. Saitoh, Y. Kawaguchi, K. Saitoh, and M. Koshiba. A design method of lithium niobate on insulator ridge waveguides without leakage loss. *Optics Express*, 19(17):15833–15842, 2011.

[17] A. Boes, L. Chang, M. Knoerzer, T. G. Nguyen, J. D. Peters, J. E. Bowers, and A. Mitchell. Improved second harmonic performance in periodically poled LNOI waveguides through engineering of lateral leakage. *Optics Express*, 27(17):23919–23928, 2019.

[18] X. R. Yu, M. K. Wang, J. H. Li, J. Y. Wu, Z. F. Hu, and K. X. Chen. Study on the single-mode condition for x-cut LNOI rib waveguides based on leakage losses. *Optics Express*, 30(5):6556–6565, 2022.

[19] R. Ulrich and R. J. Martin. Geometrical optics in thin film light guides. *Applied Optics*, 10(9):2077–2085, 1971.

[20] T. P. Shen, R. F. Wallis, A. A. Maradudin, and G. I. Stegeman. Fresnel-like behavior of guided waves. *Journal of the Optical Society of America A*, 4(11):2120–2132, 1987.

[21] M. Hammer, L. Ebers, A. Hildebrandt, S. Alhaddad, and J. Förstner. Oblique semi-guided waves: 2-D integrated photonics with negative effective permittivity. In *2018 IEEE 17th International Conference on Mathematical Methods in Electromagnetic Theory (MMET)*, pages 9–15, 2018.

[22] L. Ebers, M. Hammer, and J. Förstner. Oblique incidence of semi-guided planar waves on slab waveguide steps: Effects of rounded edges. *Optics Express*, 26(14):18621–18632, 2018.

[23] L. Ebers, M. Hammer, and J. Förstner. Light diffraction in slab waveguide lenses simulated with the stepwise angular spectrum method. *Optics Express*, 28(24):36361–36379, 2020.

[24] R. Soref. The past, present, and future of silicon photonics. *IEEE Journal of Selected Topics in Quantum Electronics*, 12(6):1678–1687, 2006.

[25] C. Vassallo. *Optical Waveguide Concepts*. Elsevier, Amsterdam, 1991.

[26] A. S. Sudbø. Film mode matching: a versatile numerical method for vector mode fields calculations in dielectric waveguides. *Pure and Applied Optics*, 2:211–233, 1993.

[27] A. S. Sudbø. Improved formulation of the film mode matching method for mode field calculations in dielectric waveguides. *Pure and Applied Optics*, 3:381–388, 1994.

[28] FIMMWAVE — Waveguide Mode Solvers. Photon Design, Oxford, United Kingdom; https://www.photond.com.

[29] M. Hammer. Oblique incidence of semi-guided waves on rectangular slab waveguide discontinuities: A vectorial QUEP solver. *Optics Communications*, 338:447–456, 2015.

[30] M. Hammer. OMS — 1-D mode solver for dielectric multilayer slab waveguides. https://www.computational-photonics.eu/oms.html.

[31] M. Lohmeyer and R. Stoffer. Integrated optical cross strip polarizer concept. *Optical and Quantum Electronics*, 33(4/5):413–431, 2001.

[32] M. Hammer. Quadridirectional eigenmode expansion scheme for 2-D modeling of wave propagation in integrated optics. *Optics Communications*, 235(4–6):285–303, 2004.

[33] E. A. Bezus, D. A. Bykov, and L. L. Doskolovich. Bound states in the continuum and high-Q resonances supported by a dielectric ridge on a slab waveguide. *Photonics Research*, 6(11):1084–1093, 2018.

[34] E. A. Bezus, D. A. Bykov, and L. L. Doskolovich. Bound states in the continuum in abruptly terminated dielectric slab waveguides. *Journal of Physics: Conference Series*, 1461(1):012204, 2020.

[35] N. Zhang and Y. Y. Lu. Non-generic bound states in the continuum in waveguides with lateral leakage channels. *Optics Express*, 32(3):3764–3778, 2024.

[36] P. Muellner, N. Finger, and R. Hainberger. Lateral leakage in symmetric SOI rib-type slot waveguides. *Optics Express*, 16(1):287–294, 2008.

[37] M. Hammer, L. Ebers, and J. Förstner. Configurable lossless broadband beam splitters for semi-guided waves in integrated silicon photonics. *OSA Continuum*, 4(12):3081–3095, 2021.

[38] E. A. Bezus, D. A. Bykov, and L. L. Doskolovich. Total absorption and coherent perfect absorption in metal–dielectric–metal resonators integrated into a slab waveguide. *Optics Letters*, 47(17):4403–4406, 2022.

[39] M. Hammer, H. Farheen, and J. Förstner. How to suppress radiative losses in high-contrast integrated Bragg gratings. *Journal of the Optical Society of America B*, 40(4):862–873, 2023.

[40] A.-S. Bonnet-Ben Dhia and F. Mahé. A guided mode in the range of the radiation modes for a rib waveguide. *Journal of Optics*, 28(1):41, 1997.

[41] Y. Plotnik, O. Peleg, F. Dreisow, M. Heinrich, S. Nolte, A. Szameit, and M. Segev. Experimental observation of optical bound states in the continuum. *Physical Review Letters*, 107:183901, 2011.

[42] Comsol Multiphysics GmbH, Göttingen, Germany; https://www.comsol.com.

[43] JCMwave GmbH, Berlin, Germany; https://www.jcmwave.com.

[44] L. Yuan and Y. Y. Lu. On the robustness of bound states in the continuum in waveguides with lateral leakage channels. *Optics Express*, 29(11):16695–16709, 2021.